Single-Walled Carbon Nanotubes -G-quadruplex Hydrogel Nanocomposite Matrixes for Cell Support Applications

Elena-Laura Ursu, Gabriela Gavril, Simona Morariu, Mariana Pinteala, Mihail Barboiu, Alexandru Rotaru

Single-Walled Carbon Nanotubes – G-quadruplex Hydrogel Nanocomposite Matrixes for Cell Support Applications

Elena-Laura Ursu[1], Gabriela Gavril[1], Simona Morariu[2], Mariana Pinteala[1], Mihail Barboiu[3] and Alexandru Rotaru[1]*

[1] *"Petru Poni" Institute of Macromolecular Chemistry, Romanian Academy, Centre of Advanced Research in Bionanoconjugates and Biopolymers, Grigore Ghica Voda Alley 41 A, 700487 Iasi, Romania.*

[2] *"Petru Poni" Institute of Macromolecular Chemistry, Romanian Academy, Electroactive Polymers and Plasmochemistry, Grigore Ghica Voda Alley 41 A, 700487 Iasi, Romania.*

[3] *Institut Europeen Membranes, Adaptive Supramolecular Nanosystems Group, Université de Montpellier, ENSCM, CNRS, Pl Eugene Bataillon, CC47, F-34095 Montpellier 5, France.*

INTRODUCTION

During the last decade supramolecular hydrogels, including self-assembled supramolecular hydrogels have received tremendous attention in the view of new materials design, preparation and applications [1–7]. These three-dimensional materials are typically constructed involving relatively weak crosslinking forces such as hydrogen bonding, metal coordination, host–guest interaction, $\pi - \pi$ interaction, etc. [8–14] An interesting direction in the design of self-assembled supramolecular hydrogels plays guanosine-based hydrogels which involve the formation of guanosine quartets as the gelation trigger [15–19]. We and others have recently considerably improved the approaches for the formation of transparent and strong guanosine-based hydrogels with high water retention values [20–22]. More precisely, the formation of boric or boronic esters has been utilized in the preparation of guanosine dimers which afterwards formed stable hydrogels in the presence of guanosine quartet stabilizing metals. Subsequently, some of the prepared hydrogels have successfully been tested as cell growing supports [22]. The cell supporting properties of guanosine diboronic hydrogels (GDH) were strictly dependent on the water retention ability of the investigated hydrogels. It was found that GDH containing Mg^{2+} and Ba^{2+} serve as better cell supports in comparison to K^+ GDH since Ba^{2+} and Mg^{2+} GDH water retention ability was three and, correspondingly fifteen times better than K^+ GDH. Unfortunately, high water retention ability of Ba^{2+} and

Mg^{2+} GDH has led to the hydrogel structure instability which resulted in difficulties of hydrogels handling during the cell experiments. Additionally, the Mg^{2+} crosslinking property has led to the strong decrease in self-assembly properties of GDH. To overcome these disadvantages, we investigated alternative crosslinking agents to both improve the GDH properties and increase the water retention. Nanofillers including clay, nanotubes or graphene oxides have already been reported to form corresponding hydrogel composites enhancing hydrogels mechanical properties by intercalation into the hydrogel polymeric or supramolecular structure [23–25]. Among the mentioned materials, carbon nanotubes (CNTs) have proved their strong efficiency in reinforcing hydrogel structures, leading to hydrogel composites with superior properties [24, 26–29]. Kouser *et al* have recently reported the facile synthesis of biocompatible nanocomposite hydrogels using microporous multi wall carbon nanotubes, dispersed chitosan, acrylonitrile N, N´-methylenebisacrylamide and linseed polyol to yield materials with significantly enhanced strength and high swelling capacity [30]. The non-toxic and biocompatible nature of the obtained materials makes them excellent candidates in the field of tissue engineering. In another study, Bellingeri et al [31] have recently investigated the properties of a novel nanocomposite made of chitosan decorated carbon nanotubes and acrylamide-co-acrylic acid hydrogels as promising substrates for biomedical applications. The new materials have shown strong pH-response, antimicrobial activity and were found to be cytocompatible. These and other examples suggested the possibility of CNT application in improving the overall properties of GDH.

In the current work, we have investigated the protocol which permits not only dispersion of single-walled carbon nanotubes (SWNTs) by GDH in liquid state, but also their successful introduction into the GDH matrix (Figure 1). The SWNTs strong impact on the overall GDH properties, including water retention ability and cytotoxicity compared to the original GDH hydrogel were investigated and described.

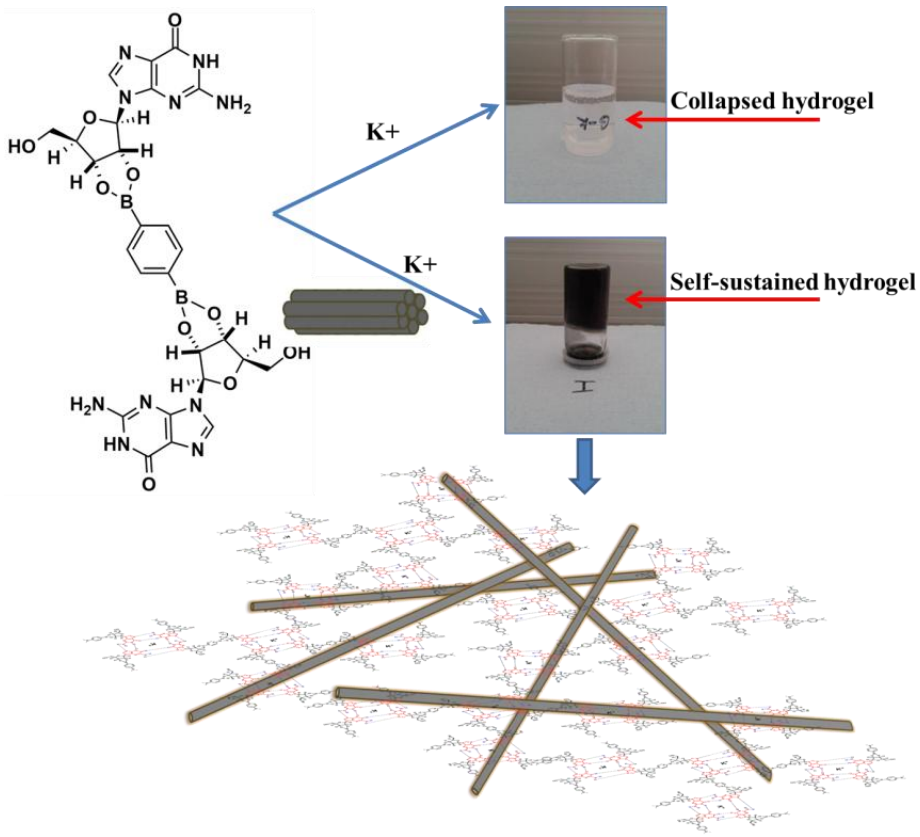

Figure 1. Schematic representation of SWNTs dispersion by GDH matrix leading to new composite hydrogels with increased water retention ability.

Moreover, the introduction of SWNTs, which is useful for the formation and stabilization of 3D supramolecular hybrid hydrogels, led to the possibility of using GDH/SWNT nanocomposites as an improved cell growing support.

MATHERIALS AND METHODS

Materials

All commercially available reagents used in the preparation of the GDH hydrogels were purchased in their highest purity grade and used without further purification. The SWNT® SG 76 single-wall carbon nanotubes obtained by catalytic chemical vapor deposition method (CoMoCAT™) were purchased from Sigma Aldrich (Munich, Germany). NHDF (normal human dermal fibroblasts) cells were acquired from PromoCell. MTS assay (CellTiter 96 AQueous One Solution Cell Proliferation Assay) was acquired from Promega.

Synthesis of GDH hydrogel-SWNT composites

GDH hydrogel-SWNT composites hydrogels were prepared utilizing an adapted synthetic protocol reported previously [22]. Thus, in a vial, an amount of 0.2 g (1 eq) of guanosine was mixed with 0.0584 g

(0.5 eq) of 1,4-benzene diboronic acid. Distilled water (7.6 mL) and 400 µL containing 0.0296 g LiOH, (1 eq, stock solution: 0.148 g in 2 mL distilled water) are added and the mixture was sonicated for several minutes until all the components were dispersed. The suspension was then heated on an oil bath preheated to 120°C until the solution becomes transparent. To avoid pressure in the vial upon heating, a syringe needle in the cap of the vial was used. After cooling to room temperature, 4 mg of SWNT were added and the solution was further sonicated to homogenously disperse the carbon nanotubes, yielding a stable black suspension. This solution was preserved and used as SWNT stock solution (SWNT-Li stock) in further experiments.

Separately, in a glass vial, 0.05g, 0.2 mmol (1 eq) of guanosine was mixed with 0.0146 g, 0.1 mmol (0.5 eq) of benzene-1,4-diboronic acid. Distilled water (1.9 mL) was added, and the mixture was sonicated for a few minutes until all the components were dispersed. The suspension was then heated in an oil bath preheated to 120^{o}C until the solution becomes transparent. To avoid pressure in the vial upon heating a syringe needle in the plastic cap of the vial was used. Next, 100 µL, 0.01 g, KOH (1 eq, stock solution of KOH: 0.66 g in 6.6 mL distilled water) was added and the mixture heated and stirred for a few more minutes, followed by the addition of the SWNT-Li stock solution (200 µL, 600 µL, 1000 µL, 1400 µL, 2000 µL, containing correspondingly 0.1 mg, 0.3 mg, 0.5 mg, 0.7 mg or 1 mg SWNT). The obtained composites were cooled down to room temperature and sonicated for 30 min to give light brown to dark black hydrogel nanocomposites.

Characterization

Water retention experiments. For each of the obtained GDH-SWNT sample, a water retention experiment was performed. Each sample was brought to the maximum water retention by the consecutive addition of water to the initial sample volume (2 mL), followed by vigorous mixing, incubation at room temperature (2 hours) and check for self-sustainability by inverting the sample vial.

Rheological measurements. The rheological properties of GDH-SWNT hydrogels were determined at 25°C on a MCR302 Anton-Paar rheometer equipped with a Peltier device. All measurements were performed using plane-plane geometry (diameter of 25 mm) and an anti-evaporation device. Firstly, the amplitude sweep tests were carried out at a constant frequency (ω) of 10 rad/s in the shear stress (τ) range of 0.001 Pa – 50 Pa, in order to determine the linear viscoelastic regime (LVR) for each sample. Then, the following tests were carried out: a) frequency sweep measurements at a constant τ value from LVR in the frequency range of 0.05 rad/s – 100 rad/s to determine the values of the storage (G') and loss (G") moduli; b) stress relaxation measurements in order to establish the gel strength; c) oscillatory step tests at 5 rad/s

carried out alternatively for 200 s at low strain (5%) and 100 s at very high strain (1000%) and the structure recovery was established in each case.

Raman spectroscopy. Raman spectra for SWNT hybrid hydrogels were recorded using an inVia Raman confocal microscope (Renishaw, UK) equipped with a He−Ne laser at 633 nm and a RenCam CCD detector coupled to a Leica DM 2500 M microscope. All measurements were performed in backscattering geometry using a 50× objective, at room temperature and atmospheric pressure.

Scanning Electron Microscopy (SEM). Morphological studies of SWNT hybrid hydrogels were performed using a Quanta 200-FEI scanning electron microscope working in low vacuum mode, at 20 kV with LFD detector. Sample of hydrogels were freeze-dried prior to measurements.

Powder X-ray diffraction (PXRD). X-ray diffraction characterization of the lyophilized samples was carried out using a D8 Advance Bruker AXS device. The X-rays were generated using a Cu Kα source with an emission current of 36 mA and a voltage of 30 kV.

MTS assay. The cytotoxicity of the GDH-SWNT hydrogels was tested in normal human dermal fibroblasts (NHDF) cells using CellTiter 96®AQueousOne Solution Cell Proliferation Assay (MTS, Promega). Cells were expanded and maintained in alpha-MEM medium (Lonza) supplemented with 10% fetal bovine serum (FBS, Gibco) and 1% Penicillin-Streptomycin-Amphotericin B mixture (Lonza) at 37°C and 5% CO2 under humidified atmosphere. For the assay, NHDF cells (PromoCell) were plated in 96-well format (5 x 10^3 cells/well in 100 µL cell culture medium) for 24 h to ensure cell adhesion. The next day the media was aspirated and replaced with the GDH solutions. For this, aliquots of 20 µL of each hydrogel (with total water volume of 5 mL) were mixed with 80 µL cell culture medium in order to obtain the desired concentrations of hydrogels. Control wells received 80 µL cell culture medium mixed with 20 µL water to ensure the control cells and the treated ones are maintained in the same conditions. Also, wells with only cell culture medium and water and wells with hydrogel solution, but/and no cells were kept in the same conditions to serve as blank values, and their additional absorbance was subtracted from the results. After 44 hours of incubation, a volume of 20 µL of CellTiter 96®AQueousOne Solution reagent was pipetted to each well and the plates were returned to the incubator. After another 4 hours the absorbance at 490 nm was recorded with a plate reader (EnSight, PerkinElmer). The cell viability was calculated and expressed as an average percentage relative to the control culture (considered 100%).

The cytotoxicity of GDH-SWNT at maximum water retention capacity (GDH (5mL), GDH-SWNTs: 0.1 mg SWNT (6 mL), 0.3 mg SWNT (7mL), 0.5 mg SWNT (9 mL), 0.7 mg SWNT (11 mL) and 1 mg

SWNT (12 mL)) and the cytotoxicity of the SWNT-Li stock was measured using the previously described protocol with the specification that in this case, aliquots of 10 μL of each hydrogel were mixed with 90 μL cell culture medium in order to obtain the desired concentrations of hydrogels. The SWNT-Li stock was diluted with cell culture medium in order to match the concentrations of the hydrogels.

GDH-SWNT cell culture studies. Aliquots of 100 μL of each hydrogel were dispensed in 96 well plates, treated with 3X TAE Mg^{2+} buffer at 7.4 pH in order to adjust the pH of the samples, followed by treatment with MEM cell culture medium to prepare the hydrogels for cell seeding. NHDF (Normal Human Dermal Fibroblasts) cells were seeded in concentration of 8 x 10^3 cells/well, using the droplet seeding technique. At this point the cells were incubated at 37°C in a humidified incubator, in order to promote cell adhesion to the surface of the hydrogel. After 4 hours, 100 μL of MEM cell culture medium was added and the samples were further incubated. At 24 hours of incubation the cells were stained using a live/dead assay. A mixture of calcein AM (5μM) and propidium iodide (500 nM) was used to selectively stain live and dead cells. After 30 minutes of incubation, in the humidified incubator, at 37°C in 5% CO_2 cells were then washed with PBS and imaged in fresh cell culture medium using an inverted Leica DMI 3000 B microscope equipped with GFP and N2.1 filters.

Additionally, a second staining protocol was used, employing the indolizinyl-pyridinium salt/β-cyclodextrin inclusion complex as a staining agent developed in our group [32]. The hydrogel samples were prepared and treated as previously described. Aliquots of 400 μL of each hydrogel were dispensed in 24 well plates. NHDF (Normal Human Dermal Fibroblasts) cells were seeded in a concentration of 5 x 10^4 cells/well, using the droplet seeding technique. After 4 hours of incubation, 400 μL of MEM cell culture medium was added and the samples were further incubated. The indolizinyl-pyridinium salt/β-cyclodextrin inclusion complex (20 μL, 3.4 mM) was added to the cell suspension at seeding time. The stained cells were subsequently imaged at 4 and 24 hours of incubation.

RESULTS AND DISCUSSIONS

In order to disperse and introduce the SWNTs inside the hydrogel structure we have developed, based on our previous expertize [22], the following strategy: first, the guanosine-boronic acid dimer solution was synthesized using standard conditions, but instead of potassium hydroxide which typically leads to the reaction and subsequent spontaneous gelation, we used lithium hydroxide which allows for the formation of the dimer but the lithium cation is not able to stabilize the guanosine quartet. Next, 4 mg of SWNTs were added and the solution (8 mL) was sonicated for 60 min to yield stable black suspension. Thus obtained SWNT-Li stock suspension was next used to introduce controlled amount of SWNTs inside the preformed GDH.

Typically, GDH were obtained using previously reported conditions [22] and the needed amount of the SWNTs was achieved by adding corresponding amounts of the SWNT-Li stock solution (equivalent of 0.1 mg, 0.3 mg, 0.5 mg, 0.7 mg and 1 mg). The obtained light-brown to black suspensions were first tested for water retention ability (Figure 2).

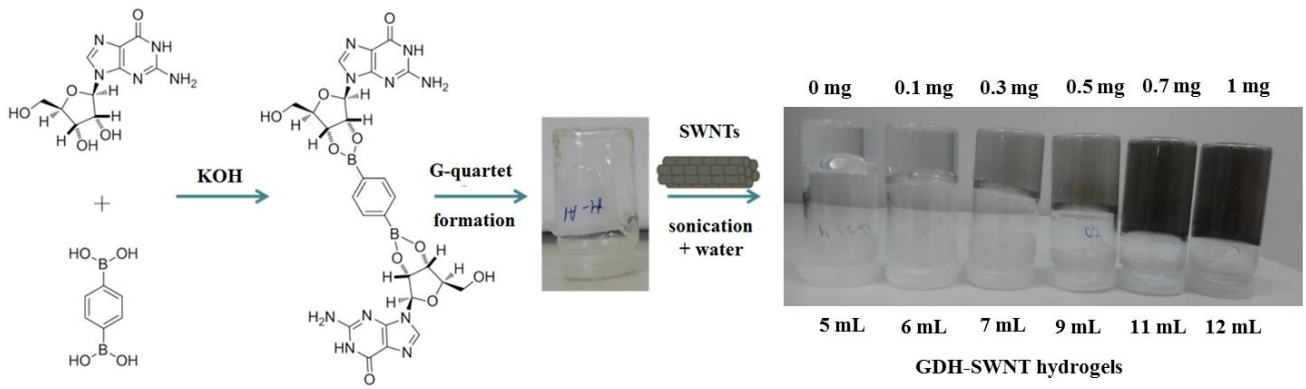

Figure 2. Water retention ability of GDH and GDH-SWNT hydrogels. The following volumes for the sample were determined: GDH (5mL), GDH-SWNT: 0.1 mg GDH-SWNT (6 mL), 0.3 mg GDH-SWNT (7mL), 0.5 mg GDH-SWNT (9 mL), 0.7 mg GDH-SWNT (11 mL) and 1 mg GDH-SWNT (12 mL).

For the investigated GDH and GDH-SWNT sample the following maximum volumes were obtained: GDH (5mL), GDH-SWNT: 0.1 mg GDH-SWNT (6 mL), 0.3 mg GDH-SWNT (7mL), 0.5 mg GDH-SWNT (9 mL), 0.7 mg GDH-SWNT (11 mL) and 1 mg GDH-SWNT (12 mL). Analyzing the obtained results we could clearly observe the increase in water retention ability (self-sustaining property) with the increase in the SWNT amount in GDH-SWNT composite hydrogels. The starting GDH was self-supportive at up to 5 mL of overall hydrogel volume, while the SWNT containing hydrogels were still self-sustained at volumes of up to 12 mL depending on the amount of SWNT. The considerable increase in water content could be explained by the reinforcing of the GDH matrix by SWNTs, leading to the combined supramolecular skeleton with pore size increasing with the absorbed water amount.

Insights on GDH and GDH-SWNT hydrogel morphology at their maximum water content were obtained by scanning electronic microscopy (SEM) on freeze-dried samples (Figure S1). The morphology of the hydrogels observed in SEM changed dramatically after the addition of first 0.1 mg of SWNTs to the GDH (Figure S1 a, b). The formation of larger distances between the agglomerations suggests the formation of larger pores inside the GDH. Interestingly, subsequent changes in the GDH-SWNT morphology with the addition of larger quantities of SWNTs were not so evident by SEM (Figure S1, c-f), the images revealing non-uniform morphologies all over the investigated surfaces. Overall, the obtained images showed a typical microporous morphology with interconnected, micrometric pores. In the case of

starting GDH the pores were denser, with smaller sizes (about 1 μm). Pore sizes proportionately increased with increasing concentration of SWNT as resultant images revealed an average pore size of 15 μm (for 1 mg of SWNT added in hydrogel).

To further confirm the implication of SWNTs into the GDH matrix and their influence on the internal π–π stacking interactions between the successive G-quartet stacks within the supramolecular hydrogel structure, we have performed the PXRD studies (Figure 4).

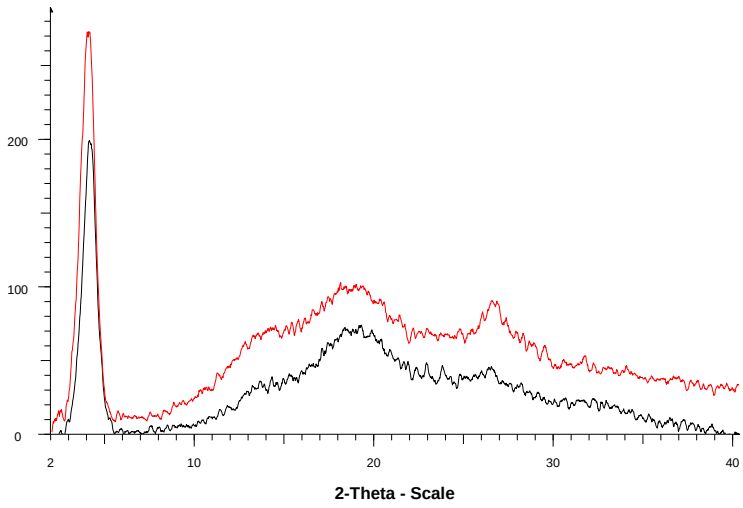

Figure 4. X-ray diffraction patterns of freeze-dried GDH (red) and GDH-SWNT composite (black) with 1 mg content of SWNTs.

The PXRD diffraction pattern of the dry GDH showed characteristic peaks at 2θ ≈ 4, 18.9 and 26.8° representing G-quartet stacks [21]. In case of GDH with the maximum amount of SWNTs (1 mg), the PXRD diffraction pattern presented similar three peaks at 2θ ≈ 4, 18.9, 26.8°, but with the slight changes in the intensity and the shifting to the lower angles of the first band, corresponding to a higher d-spacing. Additionally, an increase in the band intensity at the 2θ ≈ 26.8° was observed, owned to the overlapping of the G-quartet stacks peak and high intensity characteristic SWNTs sharp peak at 2θ = ~25° [33]. A much lower intensity of this combined peak in comparison to the reported high intensities of the individual SWNTs peak could be explained by its masking by the GDH supramolecular matrix, a phenomenon also observed in case of hydrogels containing SWNTs [34] and multi-walled carbon nanotubes [30].

To investigate the uniform incorporation of dispersed SWNTs in hydrogel structure, Raman measurements of the GDH as a reference and GDH-SWNTs with different amounts SWNTs were performed (Figure 5).

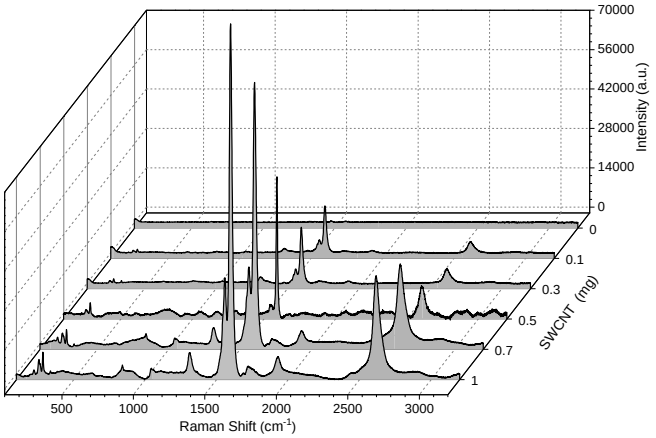

Figure 5. Raman spectra of GDH and GDH-SWNTs containing 0.1, 0.3, 0.5, 0.7 and 1 mg SWNTs.

The investigated GDH sample didn't show any signals in the investigated range between 400 and 3000 cm^{-1}. On the other hand, characteristic D-band and G-bands, as well as bands corresponding to SWNT radial breathing mode in the Raman spectra were obtained for all the investigated GDH-SWNTs, confirming the incorporation of SWNTs within hydrogel after gelation. The examined signal intensity was directly dependent on the amount of the SWNTs in the GDH matrix.

In order to confirm the gel-like behavior on the macroscopic scale of the obtained GDH-SWNTs samples and to establish their mechanical properties, rheological behavior of the composites was monitored (Figure 6). All samples have shown gel-like properties with values of the storage modulus above those of loss modulus (G' > G") (Figure 6 a). The viscoelastic moduli increased with about 3 orders of magnitude after addition of 1 mg SWNT against the original GDH. The limiting value of the shear stress, τ_L, from which hydrogels structure started to change, moved to higher values as the SWNTs content increased as a result of strong interactions developed between the components.

As shown in Figure 6 b, the frequency sweep measurements evidenced the increase of G' modulus by addition of SWNTs. Thereby, G′, determined at 1 rad/s, increases from 7.55 Pa for the sample free SWNTs to 843 Pa for that containing the maximum amount (1 mg) of SWNTs. This is consistent with the water retention data when the material holds its weight at higher amounts of water depending on SWNTs amount.

Considering the Chambon-Winter theories [35–37], for a critical gel characterized by $G'(\omega) \sim \omega^n$ and $G''(\omega) \sim \omega^n$ ($0 < n < 1$), the stress relaxation modulus G(t) shows the following power-law: $G(t)=S \cdot t^{-n}$ where n and S represent the relaxation exponent and gel strength parameter, respectively. The critical gel condition, where G' and G" were approximately parallel, was fulfilled only by the GDH-SWNTs

containing more than 0.3 mg SWNTs. S values determined by stress relaxation measurements showed an abrupt rise above 0.7 mg SWNTs (Figure 6 c).

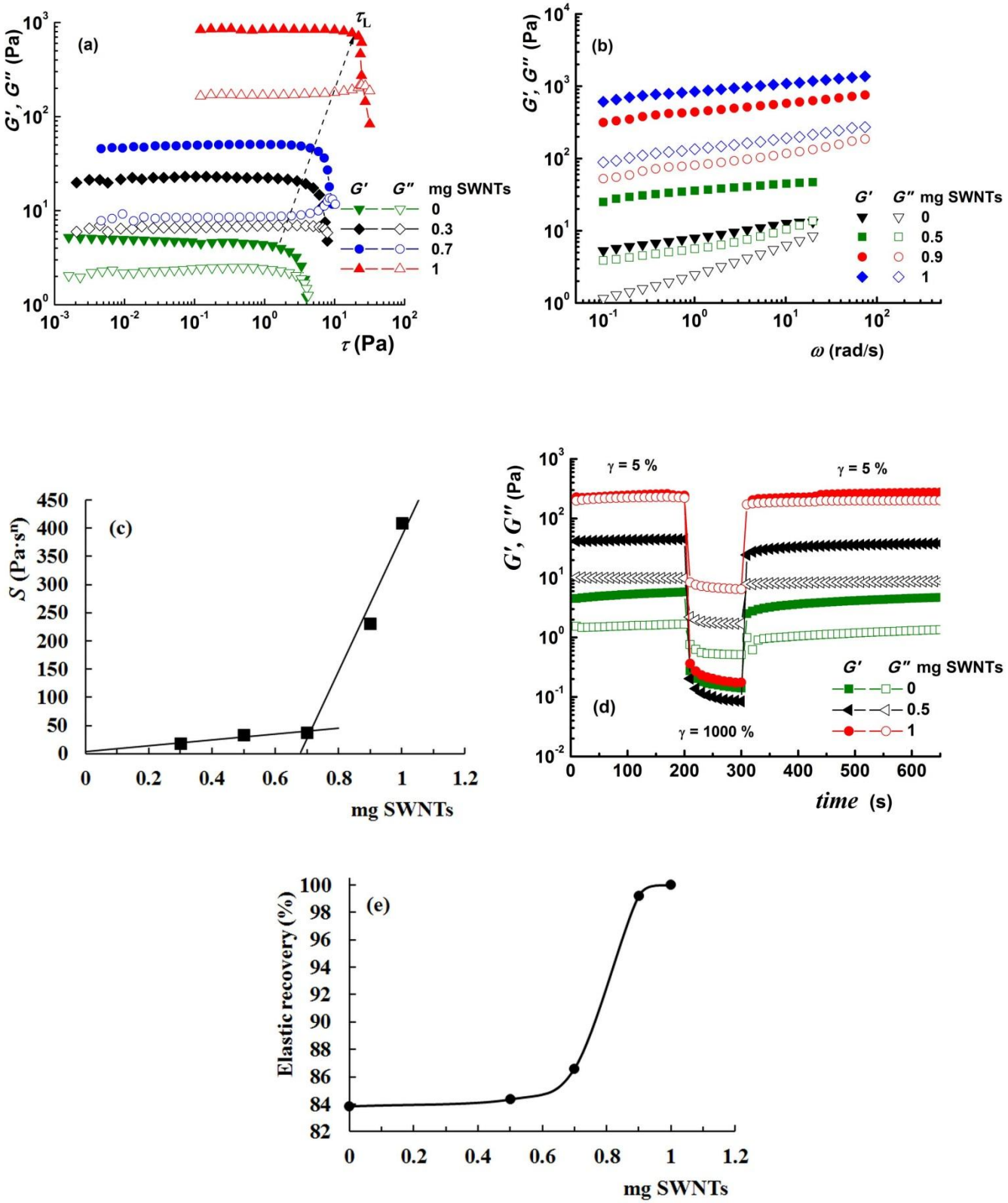

Figure 6. Rheology data: (a) variation of G' as a function of shear stress at 10 rad/s; (b) dependence of G' and G" on the oscillatory frequency in linear viscoelastic regime; (c) effect of SWNTs content on the gel strength; (d) G' and G" values in continuous step strain (5% - 1000% - 5%) measurements at 5 rad/s and (e) effect of SWNTs content on the elastic recovery.

The recovery capacity of the mechanical properties was investigated at 5 rad/s, in three consecutive steps, in which the strain (γ) is changed alternately from 5% (low strain) - 1000% (above the deformation limit) - 5%. Initially, at low strain, G' values were higher than G". By applying a high strain above a deformation limit, the network structure is broken, G" becomes higher than G' and the samples gains the liquid-like properties (Figure 6 d). When the strain returns to small value, the gel structure is recovered quickly within seconds and G' exceeds again G". In evolution of the elastic recovery degree with SWNTs content (Figure 6 e) three domains can be delimited: (*i*) up to 0.7 mg SWNTs, the elastic recovery degree remains around 84%, (*ii*) between 0.7 mg and 0.9 mg SWNTs the elastic recovery increases abruptly and (*iii*) above 0.9 mg SWNTs the regeneration of the initial structure is completely (100%). The obtained rheological data demonstrate that the GDH-SWNT hydrogels with SWNTs content greater than 0.9 mg show the superior viscoelastic properties. The insertion of the SWNTs inside the GDH matrix plays a crucial role in defining the structure and mechanical properties of these GDH samples.

After optimizing the synthesis protocol for the GDH-SWNT and the positive results obtained from characterization studies, the next step in our research was to test the hydrogels for cell supporting applications. As the original GDH showed promising results [22] in this field, we expected that the addition of SWNTs would offer an advantage in cell culture studies as the water retention capacity of the hydrogel and the overall hydrogel properties were significantly improved. First, the cytotoxicity study was performed for GDH and all GDH-SWNTs samples only at GDH maximum water retention volume (5 mL). As a result, we were able to assess the cytotoxic effect of the SWNTs in the context of the hydrogels (Figure 7).

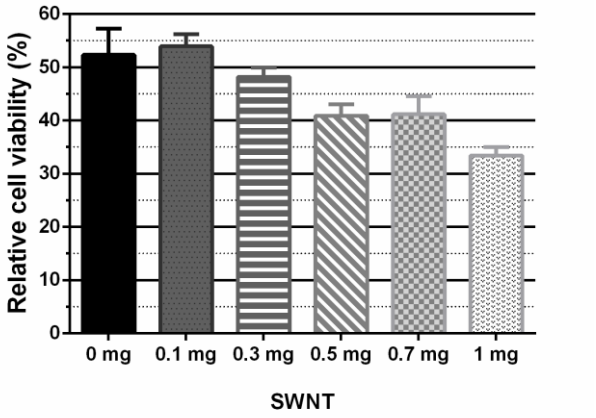

Figure 7. SWNT concentration dependence of cytotoxicity for GDH and GDH-SWNT (0.1, 0.3, 0.5, 0.7 and 1 mg SWNT) samples at a fixed volume (5 mL).

As shown in Figure 7, the increasing of SWNT in GDH from 0.1 to 1 mg led to a 20% reduction in cell viability. The decreasing in cell viability due to the presence of SWNTs was further confirmed by the evaluation of the GDH-Li and SWNT-Li solutions with corresponding amounts of SWNTs (Figure 8, grey). This experiment has clearly confirmed the cytotoxic effect of the increasing concentrations of SWNTs in comparison to the reference toxicity of the GDH-Li (100% viability). These results are in accordance with the results also reported by other researchers [38, 39].

Next, we have investigated the cytotoxicity of GDH-SWNT at maximum water retention capacity (GDH (5mL), GDH-SWNTs: 0.1 mg SWNT (6 mL), 0.3 mg SWNT (7mL), 0.5 mg SWNT (9 mL), 0.7 mg SWNT (11 mL) and 1 mg SWNT (12 mL)). The results (Figure 8, black) have revealed the fact that the increased water retention ability of the GDH given by the addition of SWNT allowed the counteraction of the SWNTs cytotoxic effect. When the water volume was increased with the increasing of SWNT concentration we can observe that the GDH-SWNTs resulted in the same cell viability percentage (70%), and most importantly the cell viability was 10% higher when compared to the starting GDH at maximum water retention capacity (Figure 8).

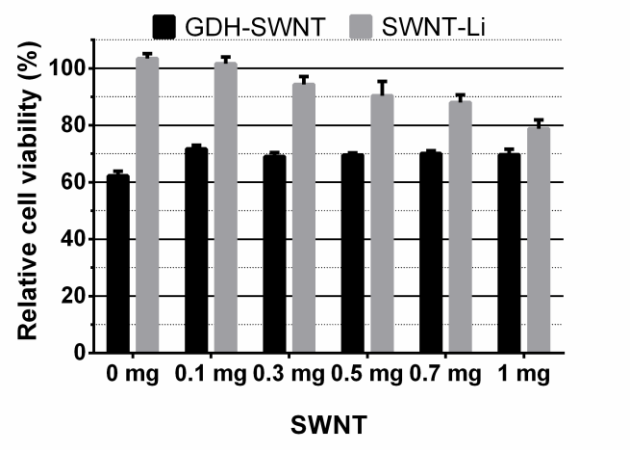

Figure 8. Cytotoxicity results for the investigated SWNT-Li suspension (grey) and GDH-SWNTs (black) with different SWNT content.

We have continued with the investigation on the cell supporting properties of the investigated GDH-SWNTs. For these studies, 6 hydrogels with increasing concentrations of SWNT with the maximum water capacity were prepared according to the established synthesis protocol. NHDF cells were cultivated on the surface of these hydrogels using the droplet seeding technique. This implies that the cells were seeded in a very small amount of culture medium (usually up to a few µL) and after it is ensured a period of up to four hours in the incubator, without adding the rest of the cell culture medium, in order to promote cell adhesion to the surface of the hydrogel. Then the rest of the cell culture medium is added and the cells are further incubated in proper conditions. Subsequently, two separate staining protocols were used and compared in these experiments. First, the live/dead assay was used as a qualitative, complementary method to the quantitative MTS assay (Figure 9). By applying this, we were able to selectively stain and visualize living cells (using calcein AM, green cells) and dead cells (using propidium iodide, red cells) in all the investigated GDH and GDH-SWNTs samples incubated with cells. The obtained pictures were then overlaid by merging the green and red fluorescence channels (using ImageJ) resulting in pictures that represent both the dead and the viable cells (Figure 9 a-f). This fluorescent staining also allowed us to better visualize the adhered cells, that otherwise would be difficult to image in bright field, since they are transparent [40]. The elongated morphology of the viable cells (green) denotes the attachment on the hydrogels surface. The pictures analysis has confirmed the results obtained in the cytotoxicity studies, showing an overwhelmingly larger number of viable cells (green) in comparison to the dead cells (red), in all the investigated samples after 24 hour of incubation.

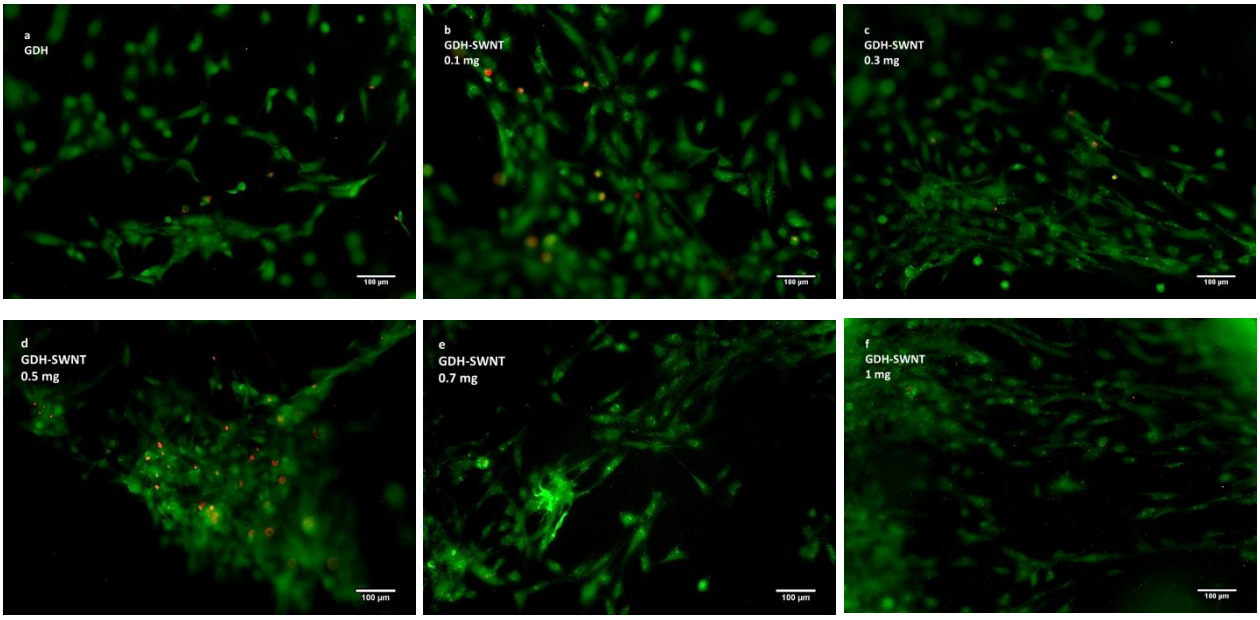

Figure 9. Fluorescence mycroscopy images of NHDF cells incubated for 24 hours and stained using live/dead assay on (a) GDH, (b-f) GDH-SWNTs at different SWNTs amounts at maximum water retention capacity.

As the fluorescence of the commercial calcein AM used to stain live cells is usually retained poorly in time [41] and could have a genotoxic effect [42] due to the exposure of samples to light during imaging, a second imaging protocol was chosen: the use of indolizinyl-pyridinium salt/β-cyclodextrin inclusion complex (IPSCD) [32] as cell staining agent developed in our group. Although this compound was developed for selective labeling of acidic organelles in cells, the absence of cytotoxicity, cellular permeability and increased long-lived intracellular fluorescence makes it a perfect candidate for imaging cells for over 24 hours without having to repeat the staining protocol. By applying this protocol, we were able to image the seeded cells at 4 and 24 hours after incubation and monitor their progress in time (Figures 10 and S2).

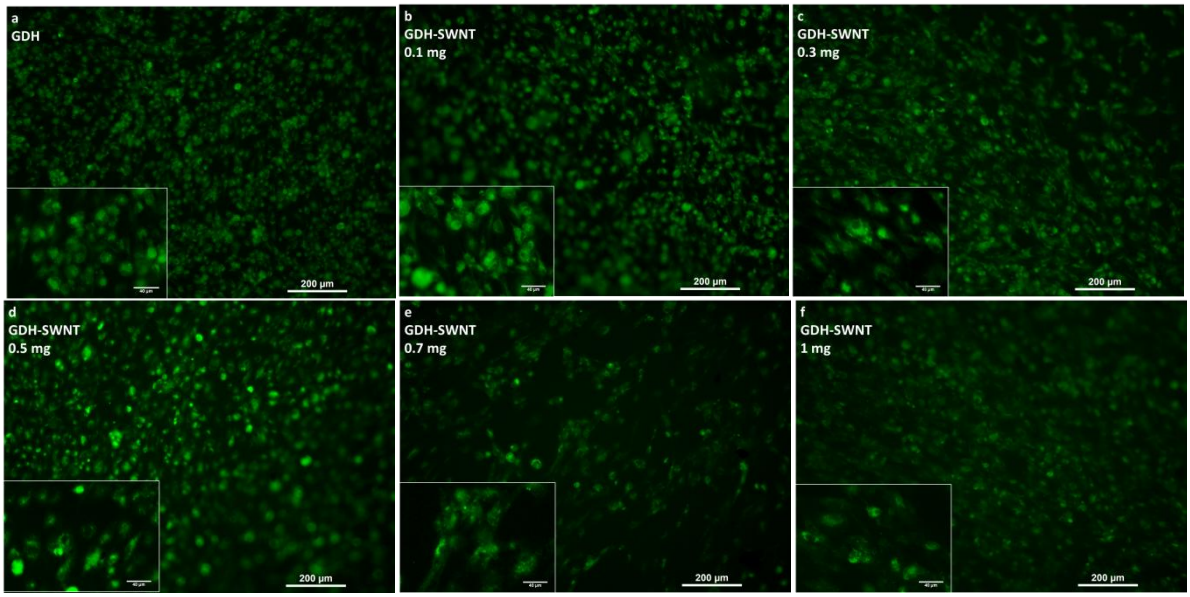

Figure 10. Fluorescence mycroscopy images of NHDF cells seeded on GDH (a) and GDH-SWNTs (b-f) after 4 hours of incubation, stained with IPSCD.

The analysis of the images obtained after 4 and 24 hours of incubation and stained with IPSCD has confirmed the results obtained by live/dead assay staining that the seeded NHDF cells were able to succesfully adhere to the surface of the hydrogels, presenting a typical fusiform appearance at all the investigated GDH-SWNTs samples.

Conclusions

We have successfully developed supramolecular GDH-SWNTs composites which exhibited much better mechanical and water retention properties compared with the starting GDH. The successful incorporation of SWNTs inside the GDH matrix was investigated by SEM, powder XRD and Raman techniques, while the hydrogels mechanical properties were in detail investigated and compared by rheological studies. The favorable cytotoxicity results for all the investigated nanocomposites and the characterization results showing an increase in the pore size after the addition of SWNTs to the GDH, made them ideal materials for cell support applications. NHDF cells have been effectively seeded and then imaged by means of two separate techniques (commercial live-dead essay and the indolizinyl-pyridinium salt/β-cyclodextrin inclusion complex essay developed in our group), showing successful attachment and cell viability in time confirmed by both utilized assays. The promising obtained results regarding cytotoxicity and cell supporting properties, together with the peculiar properties of supramolecular hydrogels to be responsive to various external stimuli, make the investigated SWNT composite hydrogels interesting materials for biomedical applications in the field of tissue engineering.

Acknowledgements

This publication is part of a project that has received funding from the European Union's Horizon 2020 research and innovation programme under grant agreement N°667387 WIDESPREAD 2-2014 SupraChem Lab. This work was also supported by a grant of the Ministry of Research and Innovation, CNCS – UEFISCDI, project number PN-III-P4-ID-PCCF-2016-0050, within PNCDI III.

References

1. Hirst AR, Escuder B, Miravet JF, Smith DK (2008) High-tech applications of self-assembling supramolecular nanostructured gel-phase materials: from regenerative medicine to electronic devices. Angew Chem Int Ed Engl 47:8002–8018. https://doi.org/10.1002/anie.200800022

2. Buerkle LE, Rowan SJ (2012) Supramolecular gels formed from multi-component low molecular weight species. Chem Soc Rev 41:6089–6102. https://doi.org/10.1039/c2cs35106d

3. Sangeetha NM, Maitra U (2005) Supramolecular gels: Functions and uses. Chem Soc Rev 34:821–836. https://doi.org/10.1039/B417081B

4. Kiyonaka S, Sada K, Yoshimura I, et al (2004) Semi-wet peptide/protein array using supramolecular hydrogel. Nat Mater 3:58–64. https://doi.org/10.1038/nmat1034

5. Lloyd GO, Steed JW (2009) Anion-tuning of supramolecular gel properties. Nat Chem 1:437–442. https://doi.org/10.1038/nchem.283

6. Dankers PYW, Hermans TM, Baughman TW, et al (2012) Hierarchical formation of supramolecular transient networks in water: a modular injectable delivery system. Adv Mater Weinheim 24:2703–2709. https://doi.org/10.1002/adma.201104072

7. Appel EA, Loh XJ, Jones ST, et al (2012) Sustained release of proteins from high water content supramolecular polymer hydrogels. Biomaterials 33:4646–4652. https://doi.org/10.1016/j.biomaterials.2012.02.030

8. Du R, Wu J, Chen L, et al (2014) Hierarchical hydrogen bonds directed multi-functional carbon nanotube-based supramolecular hydrogels. Small 10:1387–1393. https://doi.org/10.1002/smll.201302649

9. Du R, Xu Y, Luo Y, et al (2011) Synthesis of conducting polymer hydrogels with 2D building blocks and their potential-dependent gel–sol transitions. Chem Commun 47:6287–6289. https://doi.org/10.1039/C1CC10915D

10. Wang J, Lin L, Cheng Q, Jiang L (2012) A Strong Bio-Inspired Layered PNIPAM–Clay Nanocomposite Hydrogel. Angewandte Chemie International Edition 51:4676–4680. https://doi.org/10.1002/anie.201200267

11. Ma M, Kuang Y, Gao Y, et al (2010) Aromatic−Aromatic Interactions Induce the Self-Assembly of Pentapeptidic Derivatives in Water To Form Nanofibers and Supramolecular Hydrogels. J Am Chem Soc 132:2719–2728. https://doi.org/10.1021/ja9088764

12. Harada A, Takashima Y, Yamaguchi H (2009) Cyclodextrin-based supramolecular polymers. Chem Soc Rev 38:875–882. https://doi.org/10.1039/b705458k

13. Meazza L, Foster JA, Fucke K, et al (2013) Halogen-bonding-triggered supramolecular gel formation. Nature Chemistry 5:42–47. https://doi.org/10.1038/nchem.1496

14. O'Leary LER, Fallas JA, Bakota EL, et al (2011) Multi-hierarchical self-assembly of a collagen mimetic peptide from triple helix to nanofibre and hydrogel. Nat Chem 3:821–828. https://doi.org/10.1038/nchem.1123

15. Bang I (1910) Untersuchungen über die Guanylsäre. Biochemisce Zeitschrift 26:293–311

16. Gellert M, Lipsett MN, Davies DR (1962) Helix formation by guanylic acid. Proc Natl Acad Sci USA 48:2013–2018

17. Davis JT (2004) G-quartets 40 years later: from 5'-GMP to molecular biology and supramolecular chemistry. Angew Chem Int Ed Engl 43:668–698. https://doi.org/10.1002/anie.200300589

18. García-Arriaga M, Hobley G, Rivera JM (2008) Isostructural Self-Assembly of 2′-Deoxyguanosine Derivatives in Aqueous and Organic Media. J Am Chem Soc 130:10492–10493. https://doi.org/10.1021/ja8039019

19. Ciesielski A, Lena S, Masiero S, et al (2010) Dynamers at the solid-liquid interface: controlling the reversible assembly/reassembly process between two highly ordered supramolecular guanine motifs. Angew Chem Int Ed Engl 49:1963–1966. https://doi.org/10.1002/anie.200905827

20. Peters GM, Skala LP, Plank TN, et al (2014) A G4·K+ Hydrogel Stabilized by an Anion. J Am Chem Soc 136:12596–12599. https://doi.org/10.1021/ja507506c

21. Peters GM, Skala LP, Plank TN, et al (2015) G4-Quartet·M+ Borate Hydrogels. J Am Chem Soc 137:5819–5827. https://doi.org/10.1021/jacs.5b02753

22. Rotaru A, Pricope G, Plank TN, et al (2017) G-Quartet hydrogels for effective cell growth applications. Chemical Communications 53:12668–12671. https://doi.org/10.1039/C7CC07806D

23. Haraguchi K, Takehisa T (2002) Nanocomposite Hydrogels: A Unique Organic–Inorganic Network Structure with Extraordinary Mechanical, Optical, and Swelling/De-swelling Properties. Advanced Materials 14:1120–1124. https://doi.org/10.1002/1521-4095(20020816)14:16<1120::AID-ADMA1120>3.0.CO;2-9

24. Bhattacharya S, Samanta SK (2016) Soft-Nanocomposites of Nanoparticles and Nanocarbons with Supramolecular and Polymer Gels and Their Applications. Chem Rev 116:11967–12028. https://doi.org/10.1021/acs.chemrev.6b00221

25. Liu X, Miller AL, Waletzki BE, Lu L (2018) Cross-linkable graphene oxide embedded nanocomposite hydrogel with enhanced mechanics and cytocompatibility for tissue engineering. Journal of Biomedical Materials Research Part A 106:1247–1257. https://doi.org/10.1002/jbm.a.36322

26. Kovtyukhova NI, Mallouk TE, Pan L, Dickey EC (2003) Individual Single-Walled Nanotubes and Hydrogels Made by Oxidative Exfoliation of Carbon Nanotube Ropes. J Am Chem Soc 125:9761–9769. https://doi.org/10.1021/ja0344516

27. Structure of Semidilute Single-Wall Carbon Nanotube Suspensions and Gels - Nano Letters (ACS Publications). https://pubs.acs.org/doi/abs/10.1021/nl051871f. Accessed 22 Feb 2019

28. Tan Z, Ohara S, Naito M, Abe H (2011) Supramolecular Hydrogel of Bile Salts Triggered by Single-Walled Carbon Nanotubes. Advanced Materials 23:4053–4057. https://doi.org/10.1002/adma.201102160

29. Adewunmi AA, Ismail S, Sultan AS (2016) Carbon Nanotubes (CNTs) Nanocomposite Hydrogels Developed for Various Applications: A Critical Review. J Inorg Organomet Polym 26:717–737. https://doi.org/10.1007/s10904-016-0379-6

30. Kouser R, Vashist A, Zafaryab M, et al (2018) Biocompatible and mechanically robust nanocomposite hydrogels for potential applications in tissue engineering. Mater Sci Eng C Mater Biol Appl 84:168–179. https://doi.org/10.1016/j.msec.2017.11.018

31. Bellingeri R, Mulko L, Molina M, et al (2018) Nanocomposites based on pH-sensitive hydrogels and chitosan decorated carbon nanotubes with antibacterial properties. Mater Sci Eng C Mater Biol Appl 90:461–467. https://doi.org/10.1016/j.msec.2018.04.090

32. Pricope G, Ursu EL, Sardaru M, et al (2018) Novel cyclodextrin-based pH-sensitive supramolecular host–guest assembly for staining acidic cellular organelles. Polymer Chemistry 9:968–975. https://doi.org/10.1039/C7PY01668A

33. Zhou O, Fleming RM, Murphy DW, et al (1994) Defects in carbon nanostructures. Science 263:1744–1747. https://doi.org/10.1126/science.263.5154.1744

34. Materials | Free Full-Text | Solid-State Synthesis of Polyaniline/Single-Walled Carbon Nanotubes: A Comparative Study with Polyaniline/Multi-Walled Carbon Nanotubes. https://www.mdpi.com/1996-1944/5/7/1219. Accessed 22 Feb 2019

35. Winter HH, Chambon F (1986) Analysis of Linear Viscoelasticity of a Crosslinking Polymer at the Gel Point. Journal of Rheology 30:367–382. https://doi.org/10.1122/1.549853

36. Chambon F, Winter HH (1987) Linear Viscoelasticity at the Gel Point of a Crosslinking PDMS with Imbalanced Stoichiometry. Journal of Rheology 31:683–697. https://doi.org/10.1122/1.549955

37. Winter HH, Mours M (1997) Rheology of Polymers Near Liquid-Solid Transitions. In: Neutron Spin Echo Spectroscopy Viscoelasticity Rheology. Springer Berlin Heidelberg, Berlin, Heidelberg, pp 165–234

38. Cui D, Tian F, Ozkan CS, et al (2005) Effect of single wall carbon nanotubes on human HEK293 cells. Toxicology Letters 155:73–85. https://doi.org/10.1016/j.toxlet.2004.08.015

39. Manna SK, Sarkar S, Barr J, et al (2005) Single-walled carbon nanotube induces oxidative stress and activates nuclear transcription factor-kappaB in human keratinocytes. Nano Lett 5:1676–1684. https://doi.org/10.1021/nl0507966

40. Thorn K (2016) A quick guide to light microscopy in cell biology. Mol Biol Cell 27:219–222. https://doi.org/10.1091/mbc.E15-02-0088

41. Miles F, Lynch J, Sikes R (2015) Cell-based assays using calcein acetoxymethyl ester show variation in fluorescence with treatment conditions. Journal of Biological Methods 2:29. https://doi.org/10.14440/jbm.2015.73

42. Ge J, Wood DK, Weingeist DM, et al (2013) Standard fluorescent imaging of live cells is highly genotoxic. Cytometry Part A 83A:552–560. https://doi.org/10.1002/cyto.a.22291